www.bti.org.in
ISSN 0974-1453
Research article

LANTHANIDE NANOPARTICLES ENCAPSULATED POLYMER HYBRID CAPSULES FOR BIOIMAGING APPLICATIONS

Keziya James[1#], Rakhimol K.R.[1#], Sri Sivakumar[2], Sabu Thomas[1], Raji V[1*], Nandakumar Kalarikkal[1]

[1]International and Inter-University Center for Nanoscience and Nanotehnology, Mahatma Gandhi University, Priyadarsini Hills, Kottayam-686560, Kerala, India.; [2]Unit of Excellence on Soft Nanofabrication, Department of Chemical Engineering, Indian Institute of Technology Kanpur- 208016, Uttar Pradesh, , India.

[*]**Corresponding author: rakhiraj09@gmail.com, rajiiiucnn@gmail.com, rajirakhimgu@gmail.com**

[#]Both authors have equal contribution in this work.

ABSTRACT

Recently lanthanides have been used in bio-applications such as bioimaging and diagnosis due to its higher photostability and stronger luminescence. The $LaVO_4:Tb^{3+}$/ $LaF_3:Tb^{3+}$ nanoparticles were synthesized by citrate co-precipitation method. The capsules were prepared by using three polymers [Poly (allylamine hydrochloride) (PAH), Poly (styrenesulfonate) (PSS) and polyethyleneimine (PEI)] incorporated with nanoparticle. The synthesized nanoparticles were characterized by XRD, photoluminescent spectroscopy, SEM, TEM and confocal laser microscopy. XRD confirmed $LaVO_4:Tb^{3+}$/$LaF_3:Tb^{3+}$ nanoparticles of size 20.4nm and 4.678nm respectively. TEM and SEM images confirmed a hollow spherical polymer capsule structure with 5-6µm in size. The optical property of $LaVO_4:Tb^{3+}$/$LaF_3:Tb^{3+}$ nanoparticles were studied using photoluminescence spectroscopy (PL) and confocal laser microscopy at 488nm. *In vitro* cytotoxicity studies of these nanoparticles loaded capsules showed less/no cytotoxicity in comparison to the blank. Cellular uptake studies showed the uptake efficiency of capsules in HeLa cell line. The results have confirmed the biocompatibility and cellular internalization potential of $LaVO_4:Tb^{3+}$ /$LaF_3:Tb^{3+}$ (5%) nanoparticles-loaded capsules, which can be used as a suitable candidate for bioimaging and diagnostic applications.

Key Words: $LaVO_4:Tb^{3+}$ /$LaF_3:Tb^{3+}$ nanoparticles, polymer capsules, bioimaging.

INTRODUCTION

The advances in molecular and cell biology along with the development of non-invasive and high-resolution *in vivo* imaging technologies, molecular imaging has emerged as a new tool for understanding pathological changes at cellular and molecular levels. Among the nanomaterials luminescent ones become increasingly more effective biomedical tools especially for cell imaging. Nanomaterials have fascinated a great deal of interest in diverse fields, in particular drug delivery, bio-imaging and biosensing (Riehemann *et al.*, 2009). Different nanomaterials have been used in a variety of imaging applications such as near-IR optical imaging (noble metal nanoparticles-Au, Ag), X-ray computed tomography (noble metal nanoparticles-Au, Ag), magnetic resonance imaging (gadolinium and Iron based materials), fluorescence based imaging (semiconductor quantum dots, lanthanide-doped nanoparticles) etc. For diagnostic and therapeutic applications, nanoparticles must overcome a series of biological barriers such as degradation or aggregation in body fluids, crossing of the plasma membrane phagocytic clearance by reticulo-endothelial system etc so as to ultimately perform their desired function (Kievit *et al.,* 2011). Lanthanide-based nanocrystals have shown great prospective for use as luminescent materials due to electronic transitions within the 4f shell of the trivalent lanthanide ions. In particular, a very large interest in using Lanthanide-based nanoparticles (NPs) has developed because of their higher photo stability and luminescence compared to organic dyes. As a result, they are becoming highly favored for biological applications such as bio-conjugation due to their physical and optical properties. In medical and biochemical research, organic fluorescent compounds are extensively used as optical markers for proteins or nucleic acids in the study of molecular and cellular processes (Stryganyuk *et al.*, 2007).

Nowadays, microcapsules are used in many applications in the pharmaceutical, cosmetic, food, textile, adhesive, and agricultural industries (Brannon, 1993). Today, microcapsule systems have the highest potential in the pharmaceutical industry as many different necessities have to be satisfied to deliver a drug at the right moment, in the right place, and at an adequate concentration. Several approaches have been used to fabricate nanocapsules (Wasan *et al.*, 2001). One approach is to use systems that self-assemble to form capsules at given conditions, such as the aggregation of lipid molecules into spherically closed bilayer structures at low concentration, so-called vesicles or liposomes (Peyratout *et al.*, 2003). These relatively unstable structures can be in turn used as precursors for the preparation of more stable nanocapsules by crosslinking the lipid molecules. The required chemical functionalization of the lipids results in a limited applicability *in vivo*. In an analogous fashion, amphiphilic block copolymers can also combine in aqueous solution to vesicular structures (Forster *et al.,* 2002). A second approach to prepare capsules involves suspension and emulsion polymerization around latex particles. Harsh

conditions, such as prolonged alkali and acid treatments at high temperature are required to remove the latex cores (Renken *et al.,* 1998). A third method is the use of dendrimers or hyperbranched polymers for nanoencapsulation (Manna *et al.,* 2001). However, the particle preparation requires a rather costly and tedious procedure, which clearly presents a limiting factor for possible applications. Another method involves the covering of a sacrificial template core with a membrane, which is permeable for the products of subsequent core dissolution. For this approach, semipermeable polyelectrolyte complex membranes are well suited.

By engineering the physical (size and shape) and surface properties (charge, chemical and biomoities) of the nanoparticles, intracellular delivery of nanoparticles can be achieved (Zhao *et al.,* 2011; Thurn *et al.,* 2007; Chithrani *et al.,* 2006). However, this is a multistep process and sometimes the desired property may disappear due to the surface modification or aggregation of nanoparticle and reduction in the desired properties (e.g. optical, magnetic, electrical, etc). Additionally, the surface modification can be different for different types of nanoparticles. To overcome these issues, it is preferred to have a standard delivery system to deliver the nanoparticle intracellularly without any surface modification to individual nanoparticle. Moreover, the delivery system can carry the nanoparticle by avoiding direct contact of the nanoparticles with the body fluids, and thus prevent the degradation/aggregation of nanoparticles and their elimination by phagocytic cells. Fabrication of a potential nanomaterial delivery system should satisfy different tasks- the delivery system should be capable of carrying different kinds of nanomaterials in it, it should avoid physiological barriers and it should finally deliver the cargo intracellularly. To this end, we have studied the prospect of loading nanomaterials in between the polymer layers of polymer capsule and use them as effective nanomaterial delivery systems without the surface modification of individual nanoparticle.

MATERIALS AND METHODS

Cells

HeLa cell line and L929 fibroblast cell lines were purchased from National Centre for Cell Sciences (NCCS) Pune.

Synthesis of Lanthanide nanoparticles

$LaVO_4$:Tb^{3+}/LaF_3:Tb^{3+} (doped at 5% relative to the total Ln^{3+} amount) nanoparticles stabilized with citrate ligands were prepared by the citrate co-precipitation technique in aqueous solution in the presence of citrate ions (Sudarsan *et al.,* 2005). About 2g citric acid and 0.126g sodium orthovanadate/sodium fluoride were dissolved in 40 ml distilled water. The pH of the mixture was adjusted to 6 with dropwise addition of aqueous ammonium hydroxide and the solution was subsequently heated to 75^0C with stirring. About 1.094g of lanthanum nitrate hexahydrate and 0.057g of terbium nitrate (doped at 5% with respect to the total amount of lanthanide ions) were dissolved in 2 ml methanol and added dropwise to the above prepared solution which resulted in formation of white precipitate which got dissolved as the

reaction continued. After 2 h of reaction, the reaction mixture was cooled to room temperature. Subsequently 70ml ethanol was added to the reaction mixture for the nanoparticle precipitation. The particles were collected by centrifugation, washed twice with 5 ml ethanol and dried under vacuum.

Layer by layer synthesis

Three types of polyelectrolytes were used in this study: polyallylamine hydrochloride (PAH), polyethyleneimine (PEI), (both is cationic type), and polysodium 4-styrenesulfonate (PSS) (anionic type). Aqueous solutions of polyelectrolytes were prepared using 0.5M NaCl and mesoporous silica (5ε m) was used as supportive material. Mesoporous silica (10mg,) were incubated initially with PEI and washed thrice with water. This was followed by PSS (1mg/ml of 0.5M NaCl) solutions (Haider *et al.,* 2012). Then the sample was rinsed with rinsing solution to eliminate weakly bound polyanion molecules in order to avoid their reaction with oppositely charged polycation, which are deposited during the next adsorption step. Then the procedure is repeated until the required number of layers is acquired. Rinsing is required after every single deposition step. The fourth layer of capsule was layered with $LaVO_4:Tb^{3+}$ /$LaF_3:Tb^{3+}$ nanoparticles. Typically eight layers were developed and the silica core was removed by treating with 1ml of 5M hydrogen fluoride for 2 min to obtain the PSS/PAH (Fig.1).

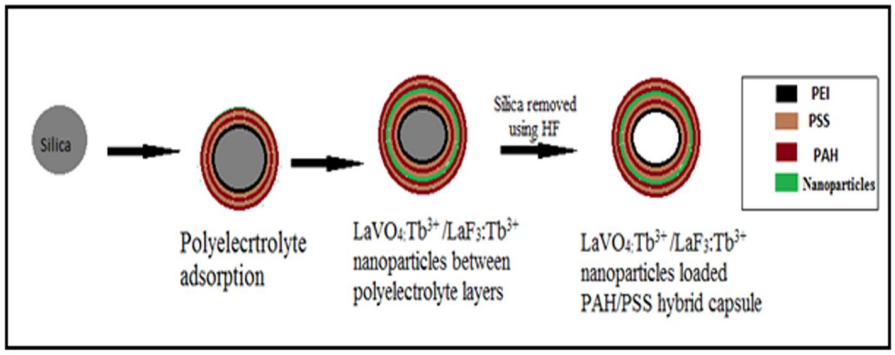

Fig.1. Schematic illustration of the polyelectrolyte deposition process for PAH/PSS capsules of the subsequent silica decomposition

Characterization of nanoparticles

The synthesized nanoparticle polymer capsules were characterized using X-ray diffraction (XRD) (Siemens D5000 Bragg- diffractometer), Photoluminescence spectroscopy (PL) (Edinburgh instruments FLSP 920 fluorescence system), Scanning emission microscope (SEM) (SUPRA 40 VP Gemini, Zeiss, Germany), Transmission electron microscope (TEM) (FEI Technai G^2 U-Twin,200 KeV) and Confocal laser scanning microscopy (Leica PCS SP5 confocal microscope,40X, oil objective).

Biocompatibility studies

L929 fibroblast cells were purchased from NCCS Pune and maintained in DMEM supplemented with 10% fetal bovine serum and allowed to grow in a humidified condition at 37^0C and 5% CO_2 atmosphere. When the cells were grown to

confluency, the medium was removed, washed with PBS and trypsinized with 0.025% trypsin in PBS/EDTA solution for 2 min and pelleted. After washing a known number of cells were seeded in 96 well plates. Different concentrations of $LaVO_4/LaF_3:Tb^{3+}$ nanoparticle loaded polymer capsules (10, 50, 100 and 200 µg/ml) were added to the cells and incubated for 24 h. After the incubation the percentage of cell viability was determined by standard cytotoxicity assays such as MTT assay and Neutral Red Uptake assay.

MTT assay (Enos *et al.,* 2010)

L929 fibroblast cells were seeded into a 96-well microtitre plate (5,000 cells/well) in 10% DMEM and incubated for 24 h. Once the cells have attached, $LaVO_4/LaF_3:Tb^{3+}$ nanoparticle loaded polymer capsules was added in different concentrations (10, 50, 100 and 200µg/ml) and incubated for 24 h at 37°C. Cells treated with 10 µg/ml concentration of Cisplatin in the same conditions were taken as positive control and another set maintained without any treatment as control. The outermost wells of the plate were avoided to reduce the drying effect. Instead, they were filled with PBS for the maintenance of humidity. After the incubation 20ε1 MTT was added to each well (5mg/ml dissolved in PBS) to each well. The plates were kept for 3 h incubation. The color developed was quantitated with an ELISA plate reader at 540nm.

The cell survival (CS) expressed as percentage was calculated as:

Per Cent cell viability = (OD NP containing capsule exposed cell / Mean OD control wells) x 100

A graph was plotted by taking percentage viability in the Y-axis and concentration of drugs in the X- axis.

Neutral Red uptake assay ((Borenfreund *et al.,* 1988)

Cells were treated with different concentrations of $LaVO_4/LaF_3:Tb^{3+}$ nanoparticle loaded polymer capsules (10, 50, 100 and 200 µg/ml) and incubated for 24 h at 37° C.. After incubation, a solution of Neutral Red, a vital dye, is added to the 96-well plate. The plates were incubated at standard culture conditions to allow neutral red uptake by the cells. After the 3 h incubation, decanted excess neutral red and PBS was added to all the wells. The solvent extracts the neutral red dye contained within the cells. The plates were placed on a plate shaker to fully extract the neutral red and evenly distribute the dye in each well and the absorbance with a 540 nm was measured using a micro plate reader. The absorbance values (OD) are then used to determine the viability of cells in each well by comparing the optical density of the each test material treated well with the negative control wells. The cell survival (CS) expressed as percentage was calculated as follows:

Per Cent cell viability = (OD NP containing capsule exposed cells/ Mean OD control wells) x 100

A graph was plotted by taking percentage viability in the Y-axis and concentration of drugs in the X- axis.

Cellular uptake studies (Haider Sami *et al.,* 2012)

The cellular uptake studies were carried out in HeLa cells grown in DMEM medium. The cells were treated with nanoparticle loaded polymer capsules and incubated at 37° C for 16 h. After incubation, the cells were washed thrice with sterilized PBS to remove excess nanoparticles and media. Then the cells were fixed using 4% formaldehyde and incubated for 20 min followed by washing thrice with PBS. To this added 200µl cytoskeleton deep orange dye to stain cytoskeleton and kept for 30 min. The dye was discarded and the samples were washed thrice using PBS. Then added 350µl Hoechst dye (Stains the nucleus to blue) and kept for 20 min. Discarded the dye and again washed thrice using PBS. Then the slides were prepared by adding a drop of glycerol and the sample containing coverslips were placed over it. The cells were observed under Confocal Laser Scanning Microscope at 488nm.

RESULTS

Synthesis and characterization

The $LaVO_4$:Tb^{3+} /LaF_3:Tb^{3+}-polymer hybrid capsules were spherical and hollow in nature. The layered nanoparticles were characterized by using different techniques for determining the characteristic properties useful for biomedical application.

X-ray diffraction was employed to determine the size of the synthesized nanoparticles. The mean particle size can be approximately determined from the broadening of the peaks by using the Scherrer equation, D = 0.941ə/ɓ cosɗ, where D is the average grain size, ə is the X-ray wavelength (0.15405 nm), ɗ and ɓ are the diffraction angle and full-width at half maximum (fwhm) of an observed peak, respectively. From the XRD data it is clear that the average particle size is 20.4 nm and 4.687 nm for $LaVO_4$:$Tb3^+$ and LaF_3:Tb^{3+} nanoparticles respectively (Fig.2).

Figure 3 shows the photoluminescence (PL) emission spectra of $LaVO_4$:Tb^{3+}/ LaF_3:Tb^{3+} nanoparticles loaded PSS/PAH capsule by excitation with laser at 488nm. The optical behavior of Tb^{3+} ion-doped nanoparticles with doping concentrations of 5% was investigated because these ions are good probes for the chemical environment of the lanthanide ions. The emission bands were observed at 544nm, 585nm and 620nm which confirm the presence of Tb^{3+} ions. The presence of nanoparticle within the polymer capsules was determined by High Resolution Transmission Electron Microscope (HRTEM). Fig.4 represents the TEM images of $LaVO_4$:Tb^{3+} /LaF_3:Tb^{3+} loaded PAH/PSS capsule. The TEM image clearly shows the polymer capsules are loaded with nanoparticles. As the image magnification increased, the nanoparticles between the polyelectrolyte layers became visible (Fig: 4b&d). In Fig. 4.a, aggregation of capsules was observed and this may be due to the drying effect during the sample preparation for TEM imaging. Hence the overall TEM images represent the spherical structure of capsules as well as the presence of $LaVO_4$:Tb^{3+} / LaF_3:Tb^{3+} nanoparticles between the PAH/PSS layers of capsules.

Scanning Electron Microscope (SEM) images were taken to understand the morphology of the polymer coated capsules with $LaVO_4$:$Tb^{3+/}$$LaF_3$:$Tb^{3+}$ nanoparticles. TEM images demonstrated the presence of

nanoparticles between the polyelectrolytes but due to aggregation, the structure of nanoparticle loaded capsules was not clear. Therefore to validate the surface morphology, the nanoparticles-loaded polymer capsules were subjected to SEM analysis. SEM images (Fig.5) of $LaVO_4:Tb^{3+}$ /$LaF_3:Tb^{3+}$ loaded PAH/PSS capsules exhibited a hollow spherical morphology with an average diameter of around 6 µm. The fluorescent property of nanoparticle was determined by using Confocal Laser Scanning microscope. About 20εl of capsule samples were fixed on a glass slide and imaged on a confocal microscope using laser with an excitation wavelength of 488 nm. The observation under 40 X objective lens showed spherical capsules with size between 5-6ε m. Also due to optical property of lanthanides, presence of each capsules were detected by green fluorescence. This observation predicts the presence of $LaVO_4:Tb^{3+}$/$LaF_3:Tb^{3+}$nanoparcticles between the layered capsules even after removal of silica using HF (Fig.6).

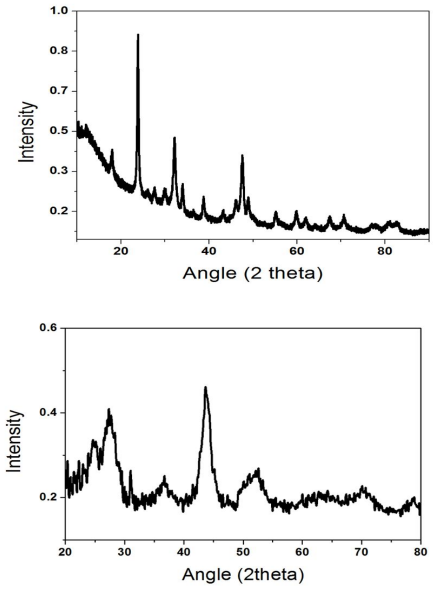

Fig.2. X-ray diffraction pattern of (a) $LaVO_4:Tb^{3+}$ nanoparticle, (b) $LaF_3:Tb^{3+}$ nanoparticle

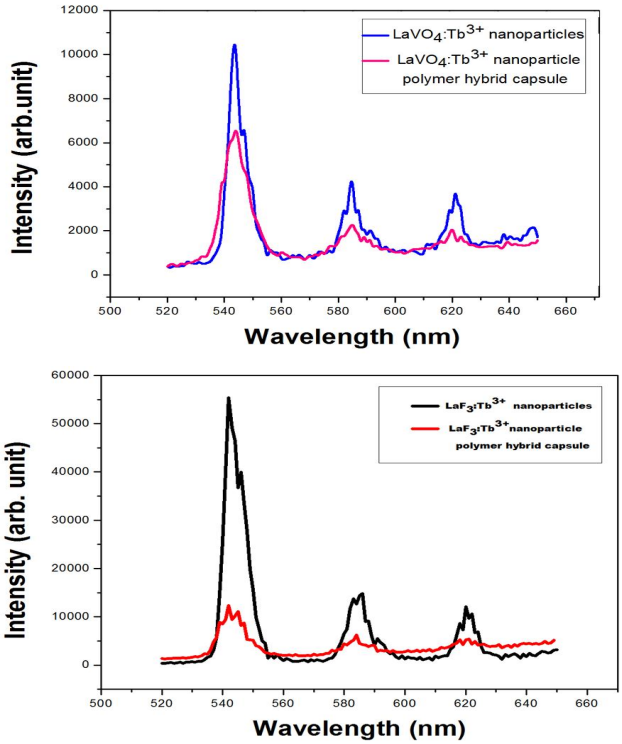

Fig.3. Photoluminescence spectra of (a) La $VO_4:Tb^{3+}$ nanoparticles and nanoparticle loaded polymer hybrid capsule and (b) $LaF_3:Tb^{3+}$ nanoparticles and nanoparticle loaded hybrid capsule excited at 488nm.

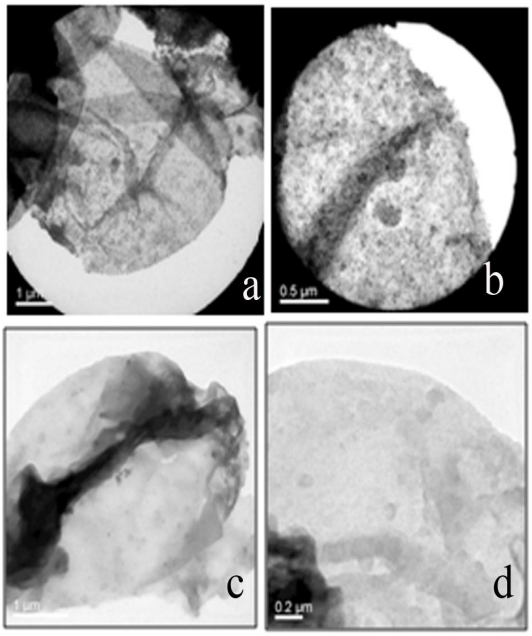

Fig.4. Transmission electron micrograph of PAH/PSS loaded polymer capsules:$LaVO_4:Tb^{3+}$(a&b), $LaF_3:Tb^{3+}$(c & d).

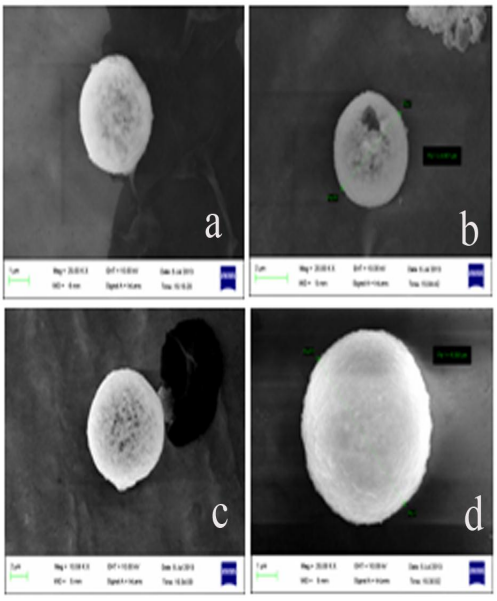

Fig.5. SEM images of: $LaVO_4:Tb^{3+}$ (a,b), $LaF_3:Tb^{3+}$ (c,d) nanoparticles capsules.

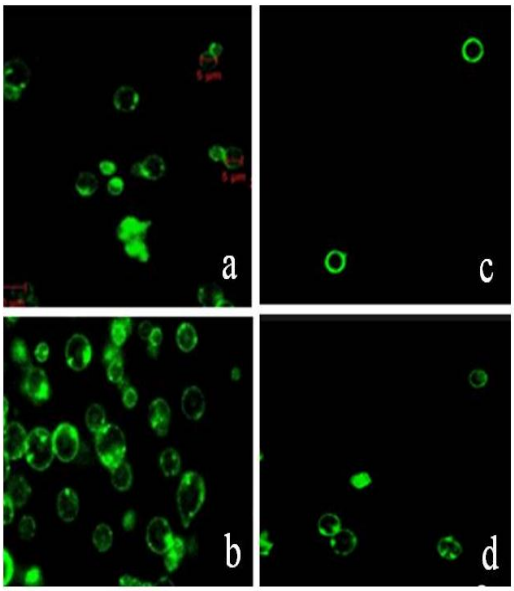

Fig.6.Confocal laser scanning image of polymer hybrid capsules loaded with loaded hybrid $LaVO_4:Tb^{3+}$ (a,b),LaF_3Tb^{3+} (c,d) nanoparticle

Biocompatibility studies

The result showed not much difference in the cell morphology by increasing the concentration of polymer hybrid capsules (Fig7). The viable cells were spindle shaped and dead cells were in irregular shape. Acute cytotoxicity of $LaVO_4/LaF_3:Tb^{3+}$ nanoparticles determined by MTT and Neutral Red Uptake assay revealed that there was no significant percentage of cell death when compared to the untreated and cisplatin treated group. After 24 h of treatment with $LaVO_4$ $/LaF_3:Tb^{3+}$- polymer capsules, the cell showed viability upto 90% for all concentrations tested (Fig.8).We found that the cell viability decreased to 67% when the concentration of $LaVO_4:Tb^{3+}$ (5%) nanoparticles were increased to 200µg/ml. This result was compared with that of cytotoxic anti-cancer drug Cisplatin treated group, which showed decrease in cell viability (50%) at a concentration of 10εg/ml. It clearly demonstrated that $LaVO_4:Tb^{3+}$ $/LaF_3:Tb^{3+}$- (5%) nanoparticles-loaded polymer capsules were non-cytotoxic on fibroblast cells at a concentration below 100εg/ml. The result of Neutral Red Uptake assay (Fig.9) also revealed the non-cytotoxicity of $LaVO_4/LaF_3:Tb^{3+}$ nanoparticles. It is evident that the $LaVO_4:Tb^{3+}$ $/LaF_3:Tb^{3+}$- (5%) nanoparticles loaded with PAH/PSS capsules showed better cell viability below 100εg/ml concentration. At lowest concentration (10εg/ml) cell viability for $LaVO_4:Tb^{3+}$ and $LaF_3:Tb^{3+}$ was 96.77 % and 93.31 respectively and is significantly comparable to the control (100%). At the highest concentration (200εg/ml), nanoparticle showed decrease in cell viability upto 67.93% for $LaF_3:Tb^{3+}$ and 73% for $LaVO_4:Tb^{3+}$. The cell death during nanoparticle treatment was compared with cisplatin treated group. At very low concentration (10µg/ml) cisplatin showed 52% cell death when compared to the control and nanoparticle treated group. The HeLa cells with nanoparticles-loaded polymer capsules showed a characteristic green emission which confirmed the presence of Tb^{3+} doped nanoparticles in a functional state inside the cell (Fig10).

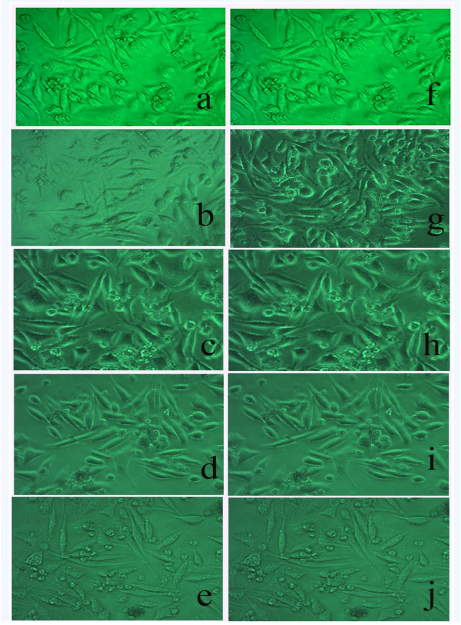

Fig7. Phase contrast microscopy, 100X, of fibroblasts cells treated with- (a & f) control, (b & g) 10 µg/ml, (c & h) 50 µg/ml, (d & i) 100 µg/ml and (e & j) 200 µg/ml] of $LaVO_4$ (a-e) and $LaF_3:Tb^{3+}$ (f-j) nanoparticles.

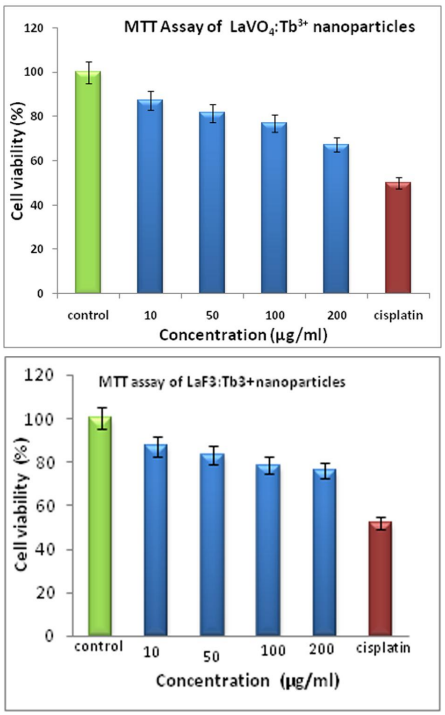

Fig 8. MTT assay of fibroblast cells showing blank and nanoparticles-loaded polymer capsules.

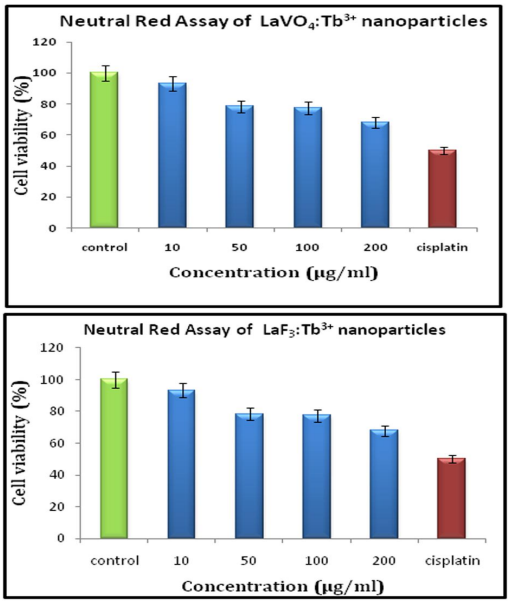

Fig 9. Neutral red uptake assay results of fibroblast cells showing blank and nanoparticles-loaded polymer capsules with varying concentration incubated for 24h.

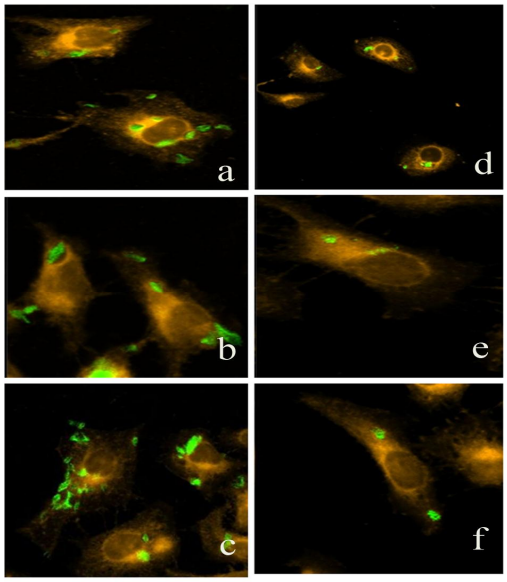

Fig.10. Confocal laser scanning microscopy (CLSM) image of HeLa cells after uptake of $LaVO_4:Tb^{3+}$ (a-c) and $LaF_3:Tb^{3+}$ (d-f) nanoparticles-loaded PSS/PAH capsule.

DISCUSSION

In this study $LaVO_4:Tb^{3+}$ /$LaF_3:Tb^{3+}$ nanoparticles were synthesized and were incorporated into the polymer capsules. The expectation was that the capsule could produce the fluorescence and hold great potential for bioimaging. The X-ray diffraction pattern of the synthesized $LaVO_4:Tb^{3+}$ /$LaF_3:Tb^{3+}$ nanoparticle showed extremely broad reflections and are due to the formation of nanosized particles, which agreed well with the reported values in the JCPDS cards (card no: 32-0504) for $LaVO_{4:}Tb^{3+}$ nanoparticle and the JCPDS cards (card no: 08-0461) for $LaF_3:Tb^{3+}$ nanoparticle respectively. Photoluminescent spectroscopy results showed the emission bands at 544, 585 and 620nm which confirm the presence of Tb^{3+} ions. Previous studies confirmed that, the emission bands around 544, 584 and 619 nm are assigned to $^5D_4$ to $^7F_5$, $^7F_4$, and $^7F_3$ transitions, respectively of Tb^{3+} ions (Haider Sami *et al.,* 2012; Zhang *et al.,* 2010). Furthermore, the optical properties of the nanoparticles-loaded capsules match with the blank nanoparticles (Fig.3.A & 3.C), which suggested that the properties of nanoparticles remain unchanged even after incorporating the polymer hybrid capsule (PAH/PSS). The strong PL properties of the luminescent nanoparticles made it easy to be identified, tracked and monitored.

Biocompatibility studies strongly recommend the use of nanoparticles for biomedical application. MTT results are in accordance with the previous result of Haider Sami *et al.* (2012), who reported non-cytotoxicity of nanoparticles loaded $LaVO_4:Eu^{3+}$ which suggests the biocompatibility of the nanoparticle for bioimaging applications. Neutral Red uptake assay confirmed the membrane integrity of cells during nanoparticle treatment. At physiological pH, the dye presents a net charge close to zero, enabling it to penetrate the membranes of the cell. Inside the lysosomes, there is a proton gradient to maintain a pH lower than that of the cytoplasm. Thus, the dye becomes charged and is retained inside the lysosomes. If the cell membrane is altered, the uptake of neutral red is decreased and can leak out, allowing for discernment between live and dead cells (Borenfreund *et al.,* 1985). An overall result predicts that the cells were capable of maintaining their pH even after treating with /$LaF_3:Tb^{3+}$- $LaVO_4:Tb^{3+}$ (5%) nanoparticles loaded with PAH/PSS capsules. Therefore neutral uptake assay confirmed $LaVO_4:Tb^{3+}$ /$LaF_3:Tb^{3+}$ (5%) nanoparticles loaded with PAH/PSS capsules to be non-cytotoxicity and biocompatible for its bioimaging application.

Cellular uptake studies confirmed the internalization of nanoparticles in cells by endocytosis. The internalized nanoparticle capsules were observed close to the nucleus which is in agreement with previous reports of Haider Sami *et al* (2012) who showed the cellular uptake efficiency of the Lanthanide nanoparticle incorporated polymer capsules in the HeLa cells. The final layer of $LaVO_4:Tb^{3+}$ /$LaF_3:Tb^{3+}$ (5%) nanoparticles capsules are PAH which is positively charged. In contrast to the low level of cell interaction and internalization by neutral and negatively charged particles, cationic particles have been well-known to

bind negatively charged groups on the cell surface and translocate across the plasma membrane. Positively charged nanoparticles, however, are most effective in crossing cell-membrane barriers and localizing in the cytosol or nucleus (Verma *et al.,* 2010). Therefore the internalization may have occurred due to charge difference between the nanoparticles loaded capsule and the cell. Cellular uptake studies thus confirmed the efficiency of $LaVO_4:Tb^{3+}/LaF_3:Tb^{3+}$-polymer hybrid capsules to enter into the cells without losing their optical properties. From these results we conclude that $LaVO4:Tb3^{+}$ $/LaF_3:Tb^{3+}$-polymer hybrid capsules are novel candidates for bioimaging applications.

ACKNOWLEDGMENTS

We greatly acknowledge UGC, Government of India for the financial support as research fellowship to Ms. Keziya James, to Biogenix Research Centre, Thiruvananthapuram, Kerala for their help in completing the biological studies.

REFERENCES

Borenfreund E, Babich H, Martin Alguacil N. (1988). Comparisons of two *in vitro* cytotoxicity assays-The neutral red (NR) and tetrazolium MTT tests, 2: 1ï 6.

Borenfreund E, Puerner J. (1985). Toxicity determined in vitro by morphological alterations and neutral red absorption. Toxicol. Lett 24:119-124.

Brannon L Peppas (1993). Controlled release in the food and cosmetic industries-Polymeric delivery system. ACS Symp. Ser.520:42 ï 52.

Chithrani BD, Ghazani AA, Chan WCW. (2006). Determining the Size and Shape Dependence of Gold Nanoparticle Uptake into Mammalian Cells. Nano Letters 6: 662ï 668.

Enos Tangke Arung, Britanto Dani Wicaksono, Yohana Ayupriyanti Handoko, Irawan Wijaya Kusuma, Kuniyoshi Shimizu, Dina Yulia, Ferry Sandra. (2010). Cytotoxic effect of artocarpin on T47D cells. J Nat Med 64:423ï 429.

Forster S and Plantenberg T. (2002). From self-organizing polymers to nanohybrid and biomaterials. Angew Chem.114:712 ï 739.

Haider Sami, Auhin Maparu and Kumar Ashok, Sivakumar Sri. (2012). Generic Delivery of Payload of Nanoparticles Intracellularly via Hybrid Polymer Capsules for Bioimaging Applications. PLos one: 7:1-12.

Kievit FM, Zhang M. (2011). Cancer Nanotheranostics: Improving Imaging and Therapy by Targeted Delivery Across Biological Barriers. Advanced Materials 23: H217ï H247.

Manna, Imae T, Aoi K, Okada M, Yogo T. (2001). Synthesis of dendrimer-passivated novel metal Nanoparticles in a polar medium: Comparison between silver and gold particles. Chem. Mater. 13:1674 ï 1681.

Peyratout C, Mohwald H, Dahne L. (2003). Preparation of Photosensitive Dye

Aggregates and Fluorescent Nanocrystals in Microreaction Containers. Adv. Mater. 15:1722ï 1726.

Renken A, Hunkeler D. (1998). Microencapsulation: a review of polymers and technologies with a focus on bioartificial organ. Polimery. 43*:* 530–539.

Riehemann K, Schneider SW, Luger TA, Godin B, Ferrari M. et al. (2009). Nanomedicine Challenge and Perspectives. Angewandte Chemie International Edition 48: 872ï 897.

Stryganyuk G *et al.* (2007). Luminescence of Ce3+ doped LaPO4 nanophosphors upon Ce3+ 4f-5d and band-to-band excitation. J of Lumi.128:355-60.

Sudarsan V, Sivakumar S, van Veggel, FC J. M, Raudsepp. (2005). General and Convenient Method for Making Highly Luminescent Sol-Gel Derived Silica and Alumina Films by Using LaF3 Nanoparticles Doped with Lanthanide Ions ($Er3^{+}$, $Nd3^{+,}$ and $Ho3^{+}$) M. Chem. Mater 17, 4736.

Thurn K, Brown E, Wu A, Vogt S, Lai B, et al. (2007). Nanoparticles for Applications in Cellular Imaging. Nanoscale Research Letters 2: 430ï 441.

Verma A, Stellacci F. (2010). Effect of surface properties on nanoparticle-cell interactions. Small 6.

Wasan KM & Drug Dev. (2001). Formulation and physiological and biopharmaceutical issues in the development of oral lipid-based drug delivery systems. Ind. Pharm.27:267 ï 276.

Zhang S, Wang L, Peng H, Li G, Chen K. (2010). Influence of P-doping on the morphologies and photoluminescence properties of $LaVO4:Tb^{3+}$nanostructures. Mater Chem Phys 123:714ï 718.

Zhao F, Zhao Y, Liu Y, Chang X, Chen C, et al. (2011). Cellular Uptake, Intracellular Trafficking, and Cytotoxicity of Nanomaterials. Small 7: 1322ï 1337.